Metal acetylene cluster ions M +(C 2H 2) n as model reactors for studying reactivity of laser-generated transition metal cations

ARTICLE *in* INTERNATIONAL JOURNAL OF MASS SPECTROMETRY · MARCH 2011

Impact Factor: 1.97 · DOI: 10.1016/j.ijms.2010.10.010

4 AUTHORS, INCLUDING:

Isaac Attah
Virginia Commonwealth University
14 PUBLICATIONS **25** CITATIONS
SEE PROFILE

M. Samy El-Shall
Virginia Commonwealth University
272 PUBLICATIONS **4,587** CITATIONS
SEE PROFILE

International Journal of Mass Spectrometry 300 (2011) 81–90

Contents lists available at ScienceDirect

International Journal of Mass Spectrometry

journal homepage: www.elsevier.com/locate/ijms

Metal acetylene cluster ions $M^+(C_2H_2)_n$ as model reactors for studying reactivity of laser-generated transition metal cations

Pramod Sharma, Isaac Attah, Paul Momoh, M. Samy El-Shall*

Department of Chemistry, Virginia Commonwealth University, Richmond, VA 23284-2006, United States

ARTICLE INFO

Article history:
Received 21 August 2010
Received in revised form 8 October 2010
Accepted 9 October 2010
Available online 16 October 2010

Keywords:
Metal ion
Acetylene
Cluster
Laser vaporization
Polymerization
Magic number

ABSTRACT

The present study explores the feasibility of utilizing acetylene clusters as model reactors for screening the catalytic activity of transition metal ions towards the polymerization of acetylene. Laser vaporization/ionization is used to generate atomic transition metal cations (M^{+*}) which interact with neutral acetylene clusters to generate $M^+(C_2H_2)_n$ cluster ions. Evidence is presented for C—H bond activation by low-lying excited states of the laser-generated V^+, Fe^+, Co^+ and Ni^+ ions. A sequential addition of acetylene molecules to the activated acetylene monomer within the clusters is proposed as a possible mechanism for polymerization of acetylene, initiated by C—H bond activation. The proposed mechanism suggests the intermediacy of $C_4H_3^+$ in the generation of higher hydrocarbon species such as $C_6H_4^+$, $C_6H_5^+$, $C_8H_6^+$ and $C_8H_7^+$. Based on thermodynamic considerations it is expected that the observed hydrocarbon ions would have cyclic structures equivalent to benzene and styrene fragments.

Enhanced ion intensities have been observed for $V^+(C_2H_2)_2$, $Cr^+(C_2H_2)_2$, $Fe^+(C_2H_2)_4$, $Fe^+(C_2H_2)_4$, $Co^+(C_2H_2)_3$, $Ni^+(C_2H_2)_3$, and $Cu^+(C_2H_2)_3$ consistent with the formation of stable covalent products formed by metal ion catalyzed polymerization of acetylene clusters. DFT calculations identify the structures of the initially formed trimer ion clusters $Fe^+(C_2H_2)_3$, $Co^+(C_2H_2)_3$ and $Ni^+(C_2H_2)_3$ where the metal cation is embedded in a "cage" created by the three acetylene molecules. Isomerization of these cluster ions into the more stable metal ion–benzene adducts is suggested and the energy needed to surpass the isomerization barriers is likely to come from the laser-generated excited state metal ions. A remarkable even–odd alternation has been observed for $Co^+(C_2H_2)_n$ clusters with enhanced ion intensities for $n = 3$, 6, 9 and 12, which could be explained by multiple isomerization events resulting in the formation of $Co^+(\text{benzene})_n$ clusters with $n = 1$–4. The combination of the excited state energy of the TM ions and the unique cluster environment which promotes concerted multi-monomer interactions with the metal ions could lead, under favorable conditions, to TM ion-mediated cyclotrimerization of acetylene molecules resulting in the formation of benzene and other polycyclic aromatic hydrocarbons.

1. Introduction

The reactivity of metal ions with small organic molecules in the gas phase has been a topic of intense investigation over the last few decades [1–9]. Interest in gas phase research of organometallic systems has advanced primarily due to the fact that the fundamental understanding obtained from these studies yields information applicable to a diverse range of fields, ranging from atmospheric chemistry to heterogeneous catalysis and interstellar chemistry. This is possible because gas phase studies can probe elementary reactions under well-defined conditions unperturbed by external factors that prevail in the condensed phase reactions such as the effects of solvent, counter ions, ion pairing, and intermolecular interactions which could lead to modification of the chemical reactions [10–12]. Moreover, these gas phase studies are also critical to identify detailed processes and mechanisms in heterogeneous catalysis [13]. For example, the majority of olefinic and acetylenic polymerization processes are catalytic, most often involving a heterogeneous catalyst [14,15]. The study of the analogous processes in the gas phase and within molecular clusters of the monomer molecules is important not only for probing the mechanism of such catalytic processes, but also for the design of new catalysts with tailored reactivity and selectivity.

A large number of studies have investigated the reactivity of transition metal (TM) cations with small organic molecules, and dehydrogenation, condensation and/or C—C bond activation have been identified as primary reaction channels [10,11,13,16–19]. These studies have revealed that TM ions are highly reactive in C—H and C—C bond activation of various hydrocarbons (including alkanes), due to the facile formation of insertion products via oxidative

* Corresponding author. Tel.: +1 804 828 3518; fax: +1 804 828 8599.
E-mail address: mselshal@vcu.edu (M.S. El-Shall).

1387-3806/$ – see front matter © 2010 Elsevier B.V. All rights reserved.
doi:10.1016/j.ijms.2010.10.010

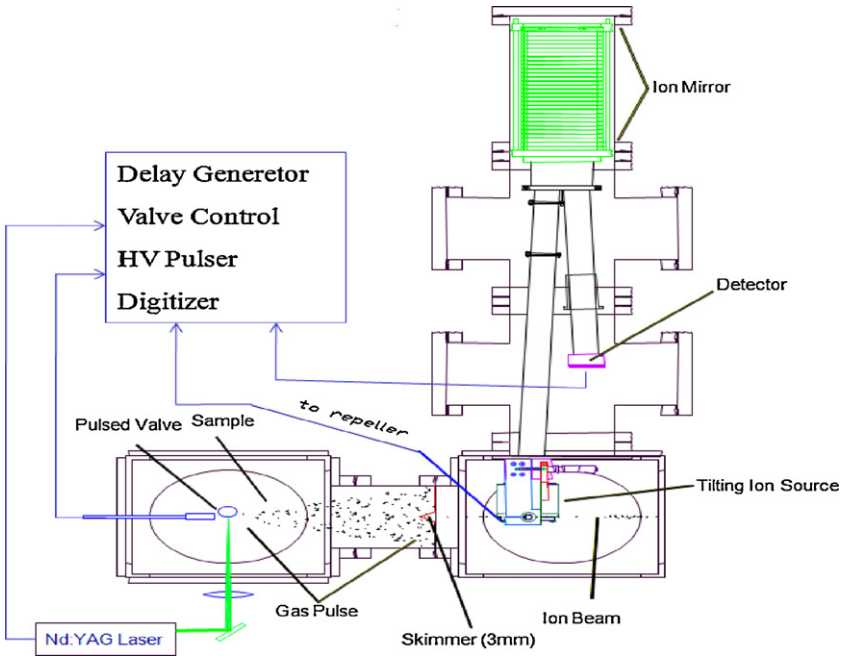

Fig. 1. Cluster beam Reflectron Time-of-Flight Mass Spectrometer (RTOF-MS) at VCU.

addition [20,21]. Thus a major motivation for these studies is the ability of the TM ions to activate otherwise inert molecules such as alkanes [22–25]. These studies have shown that the first-row groups 8–10 metal ions are more active towards C—C bond cleavage processes, whereas metal ions early in the transition series, as well as second- and third-row-metal ions, preferentially activate C—H bonds.

Cycloaddition of unsaturated hydrocarbons is a useful kind of reaction for the synthesis of aromatic hydrocarbons. Although these cyclization reactions are generally quite exothermic, they are usually hindered by high kinetic barriers as far as unactivated hydrocarbons are concerned. Due to the technological importance associated with the catalytic cycloaddition of unsaturated hydrocarbons leading to the formation of benzene and higher polycyclic aromatics, a large number of studies, both experimental and theoretical, have been carried out [26–31]. For example, Schroeter et al. [27] investigated reactions of butadiene and acetylene complexed with metal ions (Cr^+, Mn^+, Fe^+, Co^+, Cu^+) using ion-beam four-sector and Fourier transform ion cyclotron resonance mass spectrometry. It was observed that with the exception of Cu^+, for all other metal ions the reaction proceeded as a formal [4+2] cycloaddition involving 1,4-cyclohexadiene/M^+ as an intermediate, which subsequently eliminates molecular hydrogen to generate the corresponding benzene/M^+ complexes or bare M^+ and C_6H_6. Failure of Cu^+ to mediate the cycloaddition reaction was ascribed to its closed-shell s^0d^{10} electronic ground state.

Formation of benzene has also been observed in the gas phase from acetylene on Fe^+ and from ethylene on W^+ and U^+ [26,27,31]. Acetylene cyclotrimerization on supported size-selected Pd_n clusters has also been reported [32]. Various hypotheses have been formulated to explain metal ion catalyzed cyclization of unsaturated hydrocarbons leading to the formation of benzene and its analogs, but a detailed generalized mechanism is not available yet [29,31].

In this paper, we have utilized acetylene clusters containing TM atomic ions, $M^+(C_2H_2)_n$, as nano-reactors to assess the reactivity of several metal ions towards acetylene polymerization in the gas phase. The composition and abundance of $M^+(C_2H_2)_n$ as well as the hydrocarbon ions generated as a result of ion–molecule reactions within the clusters were determined using a Reflectron Time-of-Flight Mass Spectrometer (RTOF-MS). TM ions from the first, second and third rows have been studied using the Laser Vaporization Ionization (LVI) technique. Since the metals from the left side of the periodic table, i.e., V^+, Nb^+, Mo^+ and W^+ form very stable oxides, the LVI method provides a suitable and advantageous method for generating pure metal ions in the gas phase. In the present paper, we focus on the reactivity of the first row TM ions particularly Fe^+, Co^+ and Ni^+ incorporated within large acetylene clusters. In addition to the mass spectrometric studies, we also report DFT calculations on $M^+(C_2H_2)$, M = Fe, Co, and Ni for n = 1–3 aimed at elucidating and comparing the structures, binding energies, and the nature of bonding of these cluster ions with our experimental findings. The results of the second and third row TM ions will be published elsewhere. These studies have been carried out with an aim to better understand the C_2H_2 cyclotrimerization/polymerization process as well as for screening alternative efficient catalysts for polymerization of C_2H_2.

2. Experimental

The experiments were carried out on a RTOF-MS, which is based on a single stage ion mirror and 2nd order space focusing principle [33]. The system consists of two differentially pumped vacuum chambers (see Fig. 1). The first chamber, pumped by a Varian VHS-6 diffusion pump (3000 L/s in He), houses a 250 μm supersonic nozzle (General valve, series 9) for cluster production as well as a metal target for cation generation by LVI (source chamber). The second chamber (RTOF-MS chamber), pumped by a Varian VHS-4 diffusion pump (1500 L/s in He), contains the acceleration plates, flight tube, ion mirror and a microchannel-plate detector (MCP). The typical operating pressure of the source chamber and the TOF chamber are $\sim 10^{-5}$ Torr and $\leq 2 \times 10^{-6}$ Torr, respectively. For a typical experiment, the metal target is placed 0.5–1.5 cm from the nozzle face and displaced 0.5–1.2 cm from the beam axis. Acetylene clusters formed by supersonic expansion of a mixture of ~1% acetylene (BOC GASES®) in helium (ultrahigh purity, Spectra Gases, 99.99%, 4–5 atm, 250–350 μs pulse widths, 8 Hz) are interacted with transition metal cations produced by LVI of a metal target utilizing the

Table 1
Properties of transition metal cations used in this work and their role in generating hydrocarbon fragment ions from the interaction with acetylene clusters.

Metal ion	Electronic configuration	Ionization energy (eV)		Observed hydrocarbon fragments
		M^+	M^{2+}	
Ti^+	$[Ar]3d^24s^1$	6.83	13.57	×
V^+	$[Ar]3d^4$	6.74	14.61	×
Cr^+	$[Ar]3d^5$	6.76	16.48	×
Fe^+	$[Ar]3d^64s^1$	7.9	16.18	√
Co^+	$[Ar]3d^8$	7.88	17.08	√
Ni^+	$[Ar]3d^9$	7.64	18.17	√
Cu^+	$[Ar]3d^{10}$	7.72	20.29	×
Zn^+	$[Ar]3d^{10}4s^1$	9.39	17.96	×

second harmonic (532 nm) of a Nd-YAG laser (Continuum-Surelite SSP-I, 8–10 ns pulse width). For experiments with a higher seed ratio of acetylene to helium (>5%), acetylene vapor is passed over a dry ice/methanol cooled trap to remove the acetone stabilizer prior to the expansion. Under our experimental conditions the cluster generation source, as well as the laser used to generate the ions are pulsed. In addition, a pulsed high voltage is applied to the repeller plate to accelerate ions towards the detector. Hence synchronization of these different events in space as well as in time is very essential. A typical sequence begins with opening of the nozzle (t_0) which results in the generation of neutral acetylene clusters $(C_2H_2)_n$. After a certain delay (~490–550 μs), the laser Q-switch is triggered to initiate lasing, resulting in the generation of metal cations (M^+) along with anions (M^-), electrons and neutral particles. The ions subsequently interact with the neutral cluster beam forming charged clusters, $M^+(C_2H_2)_n$. The charged clusters are collimated by a 3 mm conical skimmer placed at a distance of about 4–7 cm coaxial to the nozzle. Approximately 1.05 ms after t_0, the pulse generator is triggered to supply voltage (100 μs pulses) to the repeller plate to accelerate the ions (300 V/cm) through the ion mirrors guided by the ion optics towards the MCP detector. Signal intensity is maximized by timing the laser delay so that the cations interact with the portion of the gas pulse having maximum cluster intensity and timing the pulse-generator to pulse the repeller plate at appropriate delay times. The delay generator utilized here is a BNC, model 555 generator. Data acquisition is carried out on a digital storage oscilloscope (Lecroy 9350A, 500 MHz), averaged and transferred to a computer for further processing.

The B3LYP hybrid functional [34] of the density functional theory (DFT) was utilized for all calculations employing the GAUSSIAN 03 quantum chemical package [35]. This functional has been shown to give acceptable results for geometries, binding energies, and vibrational frequencies of transition metal complexes [36,37]. All optimizations employed the 6-31+G(*d*,*p*) basis set for the C and H atoms and the Wachters + f (14s 11p 6d 3f)/[8s 6p 4d 1f] basis set for all transition metal cations [38,39]. All energies were zero point energy (ZPE) corrected and all C—H stretch frequencies were scaled by 0.96 [35].

3. Results

3.1. Observed trends within small acetylene clusters

In our first set of experiments, studies were carried out on small acetylene clusters containing metal ions of the first row transition series. These transition metals in general are widely used for various catalytic processes and represent a different order of d-shell vacancies [see Table 1]. Below we first present an overall view of the general trends observed among the reactivity of the first row TM ions followed by a more detailed study of the acetylene clusters containing Fe, Co and Ni ions. We then present the structural calculations of the $M^+(C_2H_2)_n$ clusters for M = Fe, Co and Ni, and n = 1–3. Finally, we discuss the experimental observations in relation to the structural calculations and present a plausible reaction mechanism to explain the observed trends.

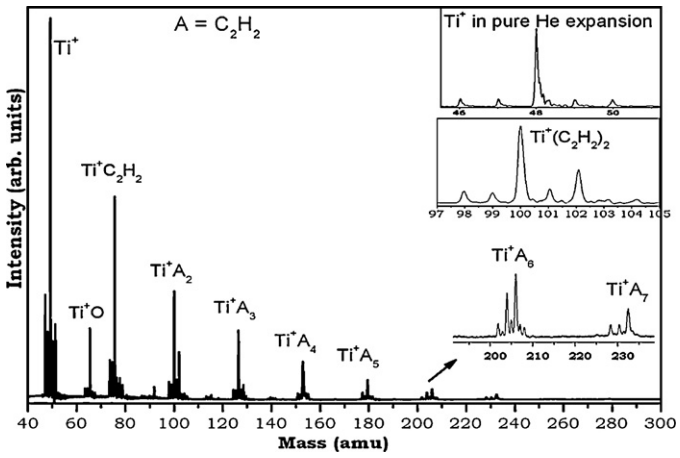

Fig. 2. TOF mass spectrum of $Ti^+(C_2H_2)_n$ clusters. Insets show the mass spectra of different isotopes of Ti^+ generated in pure helium expansion (no acetylene) and $Ti^+(C_2H_2)_2$ cluster (high resolution).

Figs. 2–4 represent the RTOF-MS spectra obtained upon the interaction of acetylene clusters with the Ti^+, V^+ and Cr^+ ions. The major cluster series observed is $M^+(C_2H_2)_n$ with n up to 8, 7 and 10 for the Ti^+, V^+ and Cr^+ ions, respectively. No other side-products arising as a result of intracluster reactions within the $M^+(C_2H_2)_n$ clusters were observed for Ti^+- and V^+-containing clusters However, for $V^+(C_2H_2)_n$ clusters hydrogen abstraction reactions were observed resulting in the generation of $V^+C_{2n}H_{2n-m}$ species (see

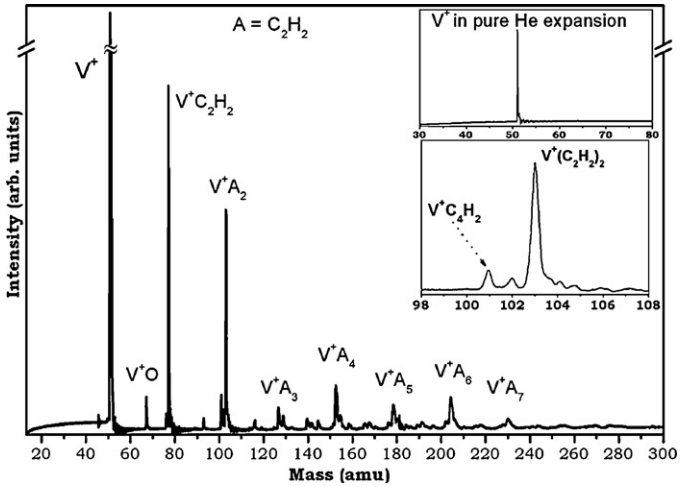

Fig. 3. TOF mass spectrum of $V^+(C_2H_2)_n$ clusters. Insets show the mass spectra of V^+ in pure helium expansion (no acetylene), and $V^+(C_2H_2)_2$ cluster (high resolution).

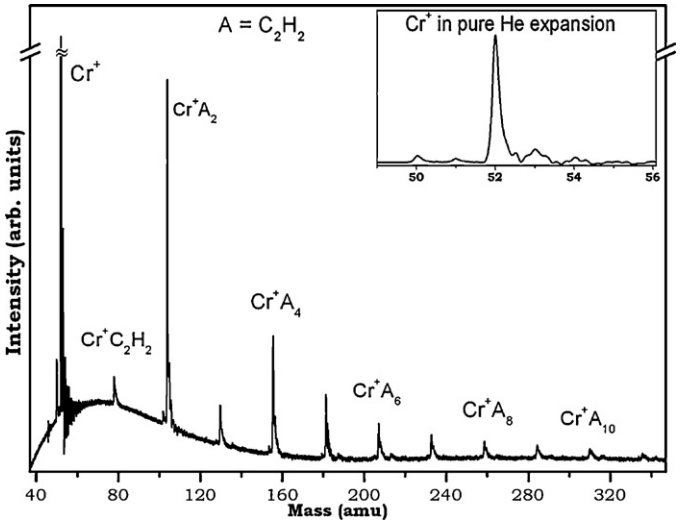

Fig. 4. TOF mass spectrum of $Cr^+(C_2H_2)_n$ clusters. Inset shows the mass spectrum corresponding to different isotopes of Cr^+ generated in pure helium expansion (no acetylene).

Fig. 3, inset) according to:

$$V^+(C_2H_2)_n \rightarrow V^+C_{2n}H_{2n-m} + \frac{m}{2}H_2 \quad (1)$$

A drop in the ion intensity is observed for the $V^+(C_2H_2)_n$ clusters after $n = 2$, which could be attributed the stability of the $n = 2$ cluster.

Figs. 5–7 display the mass spectra of the $M^+(C_2H_2)_n$ clusters for M = Fe, Co and Ni, respectively. For the three metal cations, clusters with n in the range 1–15 were observed. In addition, ion signals corresponding to hydrocarbon fragments were also observed. These ions are believed to be covalently bonded hydrocarbon fragments formed as a result of metal ion induced catalytic polymerization, as previously reported by Schwarz and co-workers for the case of Fe^+ [26–28]. It should be noted that the intensity of the observed hydrocarbon ions increases when the metal target is placed closer to the nozzle as shown in the mass spectrum of $Co^+(C_2H_2)_n$ displayed in Fig. 6b. This suggests that excited state ions could be responsible for the reactions leading to the generation of these hydrocarbon ions. TM ions are characterized by a large number of low-lying electronic states that can be easily accessed under the typical LVI conditions as was recently studied by ion mobility [40]. In fact, the geometry of the ion source plays an important role in the extent of excited state ions generated by the LVI process [40]. By placing the metal target very close to the nozzle, the gas expansion pulse overlaps efficiently with the laser plume where the density of the excited state TM metal ions is high. This increases the probability of excited state metal ion reactions with the acetylene clusters. The possible role of excited state ions in the generation of the observed hydrocarbon ions will be addressed in Section 4.

For $Co^+(C_2H_2)_n$ and $Ni^+(C_2H_2)_n$ clusters, a sharp drop in ion intensity is observed following the $n = 3$ cluster while for $Fe^+(C_2H_2)_n$, enhanced intensity is observed for $n = 4$ with a drop in ion signal for clusters with $n > 4$.

A significant enhanced ion intensity is observed for the $n = 3$ of the $Cu(C_2H_2)_n^+$ clusters with no side-products assigned to hydrocarbon fragments as shown in Fig. 8. Similarly, with Zn^+ the major ions observed belong to the $Zn(C_2H_2)_n^+$ cluster series although the overall clusters' ion signal is much weaker compared to other TM ions (Fig. 9).

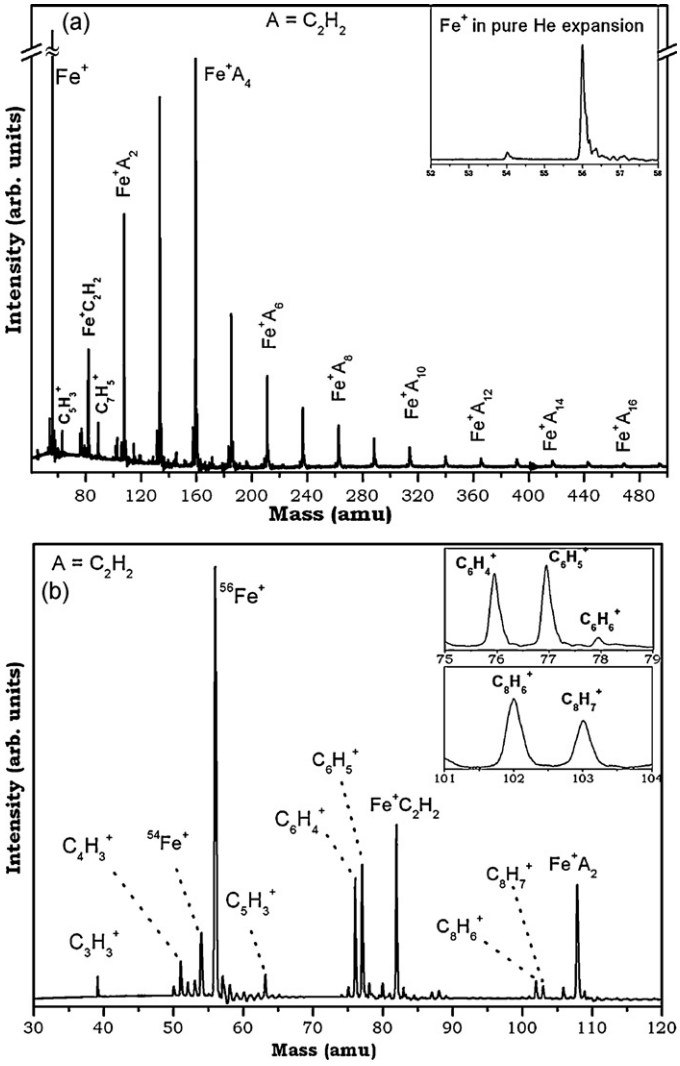

Fig. 5. (a) TOF mass spectrum of $Fe^+(C_2H_2)_n$ clusters. Inset shows the mass spectrum of Fe^+ in pure helium expansion (no acetylene). (b) TOF mass spectrum of the hydrocarbon ions generated from the $Fe^+(C_2H_2)_n$ clusters. Insets show mass spectra of the $C_6H_4^+$, $C_6H_5^+$, $C_6H_6^+$, $C_8H_6^+$, and $C_8H_7^+$ ions (high resolution).

3.2. Fe^+, Co^+ and Ni^+ ions in large acetylene clusters

To investigate the magic numbers' behavior within large $Fe^+(C_2H_2)_n$, $Co^+(C_2H_2)_n$ and $Ni^+(C_2H_2)_n$ clusters, we generated these clusters by increasing the stagnation pressure of the He carrier gas and by increasing the seed ratio of acetylene during the supersonic beam expansion to produce large neutral acetylene clusters. The interaction of these clusters with the metal cations generated by the LVI process is maximized by increasing the laser delay so that the cations interact with the portion of the gas pulse having the larger neutral clusters and then pulsing the repeller plate at appropriate delay times to detect the corresponding cluster ions.

The mass spectra of the large $Fe^+(C_2H_2)_n$, $Co^+(C_2H_2)_n$ and $Ni^+(C_2H_2)_n$ clusters are displayed in Fig. 10a–c, respectively. The insets display the corresponding intensity plots. The observed features in the small $Fe^+(C_2H_2)_n$ clusters (Fig. 5a) are more pronounced within the larger acetylene clusters. For example, the mass spectrum displayed in Fig. 10a shows enhanced intensity for the $Fe^+(C_2H_2)_2$ and $Fe^+(C_2H_2)_4$ clusters. The enhanced intensity of the $Fe^+(C_2H_2)_2$ cluster could suggest stabilization of the acetylene dimer by a highly symmetric Fe^+-bisacetylene arrangement or formation of a covalent Fe^+-dimer complex, i.e., $Fe^+C_4H_4$. As will

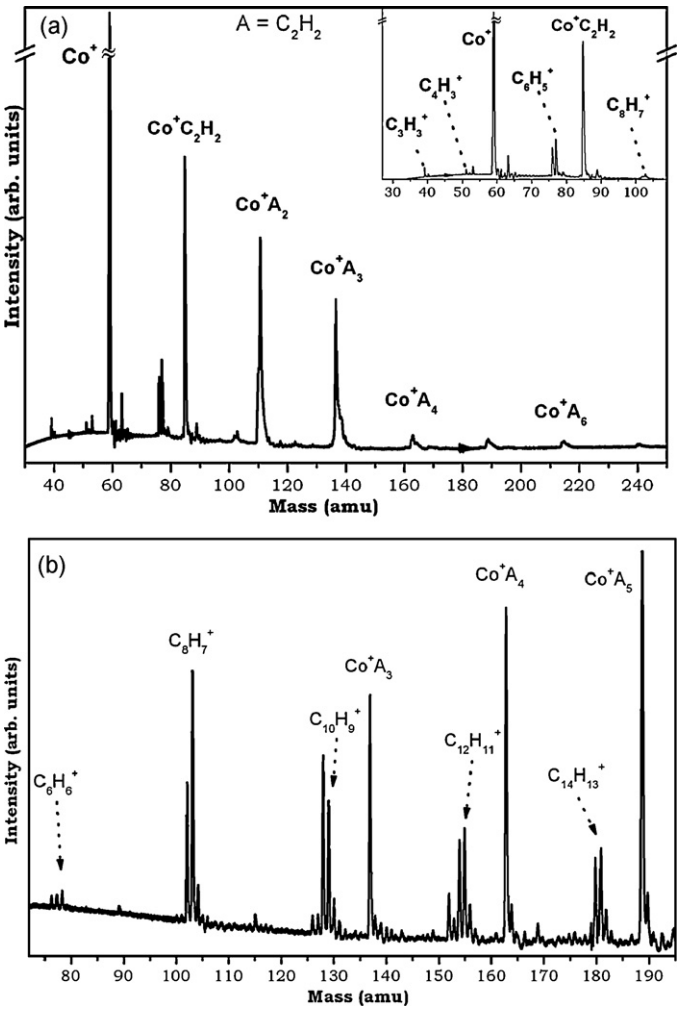

Fig. 6. (a) TOF mass spectrum of $Co^+(C_2H_2)_n$ clusters. Inset shows the mass spectrum of the hydrocarbon ions generated from the $Co^+(C_2H_2)_n$ clusters. (b) TOF mass spectrum of hydrocarbon ions generated from the $Co^+(C_2H_2)_n$ clusters when the Co target is placed closer to the nozzle generating the $(C_2H_2)_n$ clusters.

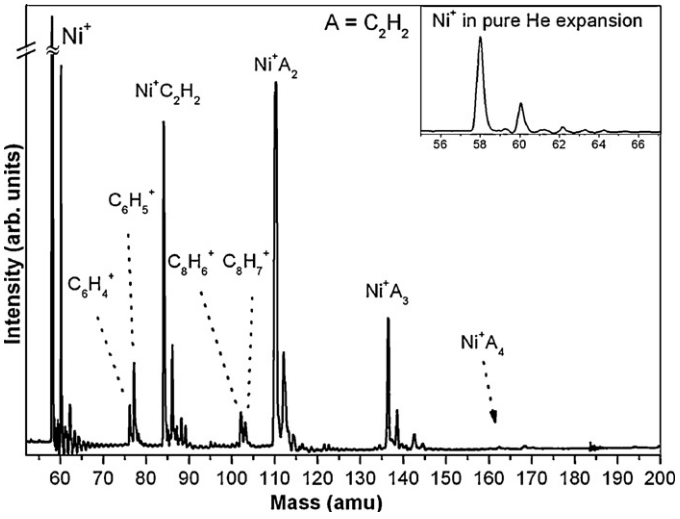

Fig. 7. TOF mass spectrum of $Ni^+(C_2H_2)_n$ clusters. Inset shows the mass spectrum of Ni^+ in pure helium expansion (no acetylene).

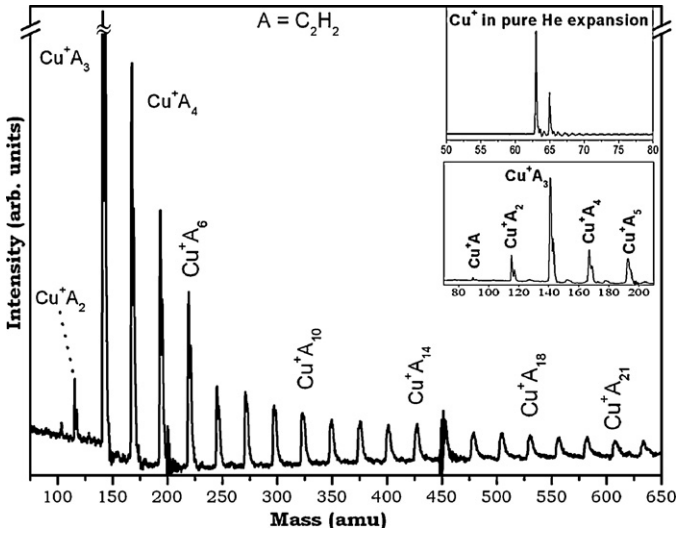

Fig. 8. TOF mass spectrum of $Cu^+(C_2H_2)_n$ clusters. Insets show the mass spectra of Cu^+ in pure helium expansion (no acetylene), and $Cu^+(C_2H_2)_3$ cluster (suggested magic number).

be discussed later, DFT calculations suggest the Fe^+-bisacetylene geometry to be more stable than the $Fe^+C_4H_4$ complex. The enhanced intensity of the $Fe^+(C_2H_2)_4$ cluster could suggest that four acetylene molecules are required for closing the first solvation shell of the Fe^+ cation. However, it should be mentioned that the $n = 4$ cluster does not necessarily represent the cation coordination number but rather stability from efficient ligand packing.

Inspection of the mass spectrum of the larger $Co^+(C_2H_2)_n$ clusters (Fig. 10b) reveals a remarkable and reproducible trend; oscillatory magic numbers for the $n = 3$, 6, 9, and 12 clusters. This pattern is also consistent with the distribution of the small $Co^+(C_2H_2)_n$ clusters which shows a sharp drop in ion intensity after the $n = 3$ cluster (Fig. 6). It is tempting to speculate that a Co^+-mediated multiple intracluster reaction process could be occurring in which a benzene ring and other covalent C_6H_6 products (perhaps multiple cyclic rings $Co^+(C_6H_6)_n$, $n = 1$–4) are formed. This possibility is of interest since it provides further evidence for intracluster reactions enhanced by interactions among the packed reactive molecules in the cluster. However, using FT-ICR mass spectrometry, Schwarz and Wesendrup concluded that the cobalt cation was

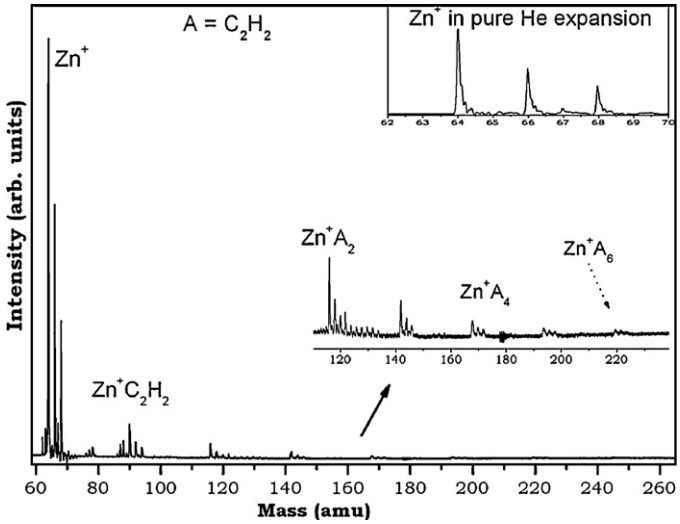

Fig. 9. TOF mass spectrum of $Zn^+(C_2H_2)_n$ clusters. Inset shows the mass spectra of Zn^+ in pure helium expansion (no acetylene).

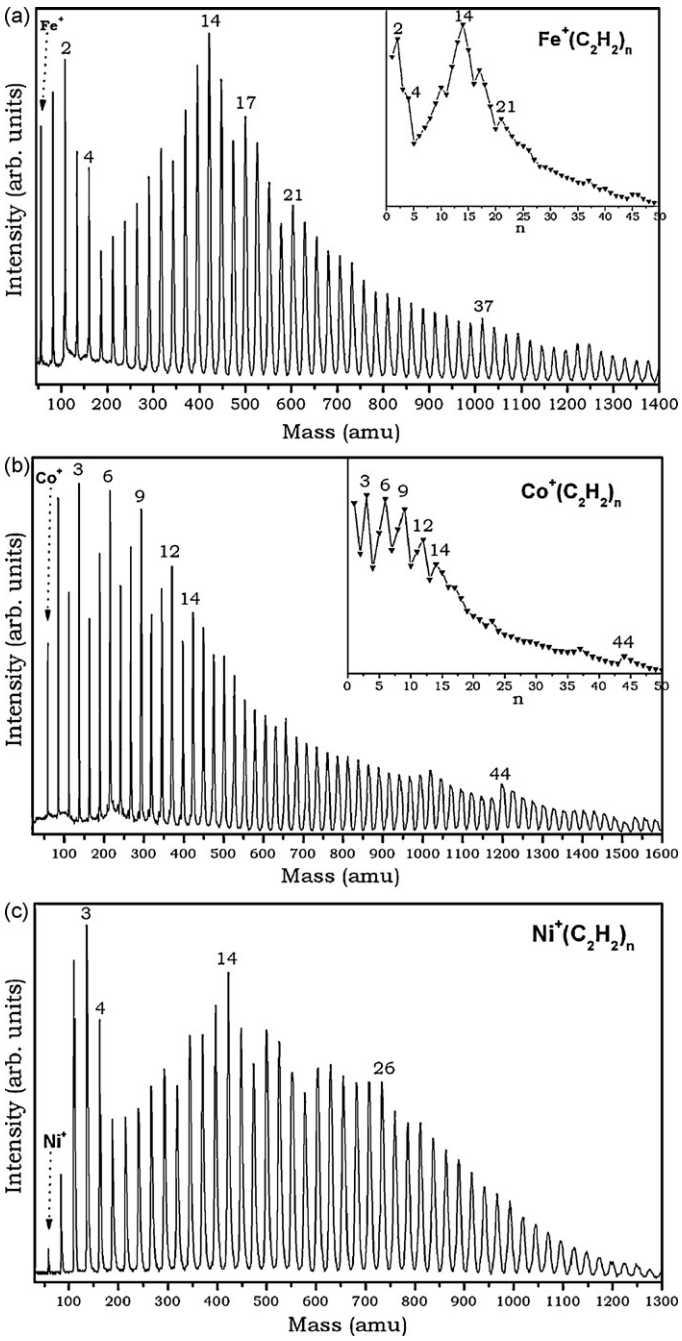

Fig. 10. (a) TOF mass spectrum of large $Fe^+(C_2H_2)_n$ clusters. The neutral acetylene clusters were generated by the supersonic beam expansion of 3% acetylene/helium mixture (100 psi). Laser fluence at the Fe target surface was $\approx 10^7$ W cm^{-2}. Inset shows the corresponding intensity plot suggesting magic numbers at $n = 2$, 4 and 14. (b) TOF mass spectrum of large $Co^+(C_2H_2)_n$ clusters. The neutral acetylene clusters were generated by the supersonic beam expansion of 3% acetylene/helium mixture (100 psi). Laser fluence at the Co target surface was $\approx 10^7$ W cm^{-2}. Inset shows the corresponding intensity plot suggesting intriguing magic numbers at $n = 3$, 6, 9 and 12. (c) TOF mass spectrum of large $Ni^+(C_2H_2)_n$ clusters. The neutral acetylene clusters were generated by the supersonic beam expansion of 3% acetylene/helium mixture (100 psi). Laser fluence at the Ni target surface was $\approx 10^7$ W cm^{-2}.

unreactive in regards to mediation of the acetylene cyclotrimerization reaction [28]. In fact, most late first-row transition metal cations with the exception of iron are not expected to mediate the cyclotrimerization reaction. We therefore suspect the Co^+-mediated cylotrimerization reaction to be a consequence of excited state Co^+ ions reacting with acetylene molecules in the $Co^+(C_2H_2)_n$ large clusters. This could provide the energy needed to surpass the barrier involved in the isomerization of the $Co^+(C_2H_2)_3$ cluster species into the more stable Co^+-benzene structure. Dissipation of excess energy resulting from the exothermic cylotrimerization reaction occurs via evaporative loss of neutral acetylene molecules, a process that is favored in a large cluster distribution [41]. It is well established that a cluster environment, much like the condensed phase, increases the rate of certain termolecular processes which may otherwise be inefficient under gas phase conditions [41–43]. It should be mentioned that at the experimental pressures ($\ll 5 \times 10^{-8}$ bar) utilized by Wesendrup and Schwarz [28], the probability of orientational collisions amenable to efficient Co^+-mediated trimerization reaction kinetics might be too low. Cluster size-specific TM-mediated intracluster reactions may also be responsible for the observed magic numbers [44].

For the large $Ni^+(C_2H_2)_n$ clusters (Fig. 10c), the $n = 3$ cluster shows enhanced intensity consistent with the spectrum of the small clusters (Fig. 7) which could suggest a particularly stable structure for this cluster. The enhanced $n = 3$ cluster is suspected to result from efficient packing of three acetylene molecules around the nickel cation. Another possibility is a Ni^+-mediated intracluster cyclization reaction resulting in the formation of a Ni^+(benzene) structure similar to the suggested process in the $Co^+(C_2H_2)_n$ clusters. Using IR dissociation experiments, Duncan and co-workers suggested the Ni/trimer geometry to be analogous to that of the tris(ethylene)platinum complex [44]. They suggested four acetylene molecules are needed to close the Ni^+ first solvation shell, and proposed that the Ni-cyclobutadiene π-complex ($Ni^+C_4H_4$) is formed in larger clusters from a size-specific intracluster reaction [44]. These suggestions are in full agreement with our mass spectra data where an enhanced intensity peak for $Ni^+(C_2H_2)_4$ is observed (Fig. 10c).

Another observation common to the $Fe^+(C_2H_2)_n$, $Co^+(C_2H_2)_n$ and $Ni^+(C_2H_2)_n$ clusters and other metal ions containing acetylene clusters as well is the appearance of a magic number at $n = 14$ (Fig. 10a–c). This magic number is attributed to an icosahedral structure, composed of a strongly bound central $M^+(C_2H_2)_2$ cation surrounded by 12 neutral acetylene molecules in an icosahedral arrangement consisting of two staggered 5-membered rings along the equator with each pole capped by another molecule [45,46]. This assumption is consistent with the observed strongly bound $M^+(C_2H_2)_2$ clusters as confirmed by the theoretical calculations. It should be noted that extensive evaporation of acetylene molecules is expected upon the interaction of the hot metal ions and the cold acetylene clusters. Intracluster exothermic reactions induced by the metal ions also result in neutral evaporation. These evaporation events result in magnifying the small differences in the binding energies among the cluster ions since relatively strong bound clusters experience less evaporation. In the present system, the binding of the "outer" acetylene molecules is expected to be by mere van der Waals interaction approximately similar to the binding energy of the neutral acetylene dimer (≈1.16 kcal/mol) [47]. Although the assumption of a strongly bound $M^+(C_2H_2)_2$ core ion surrounded by 12 neutral acetylene molecules is appealing and provides a plausible explanation of the observed $n = 14$ magic number for the $M^+(C_2H_2)_2$ clusters, it lacks direct experimental and theoretical evidence.

3.3. Structural calculations of $M^+(C_2H_2)_n$ clusters for M = Fe, Co and Ni, and n = 1–3

Fig. 11 shows the DFT calculated structures of the $M^+(C_2H_2)_n$ clusters for M = Fe, Co and Ni, and $n = 1$–3. The calculated binding energies, vibrational frequencies (C—H symmetric and asymmetric stretch), bond lengths and angles are given in Table S1 (Supplementary data); along with corresponding values predicted from previous calculations [37,48,49]. The optimized geometries show

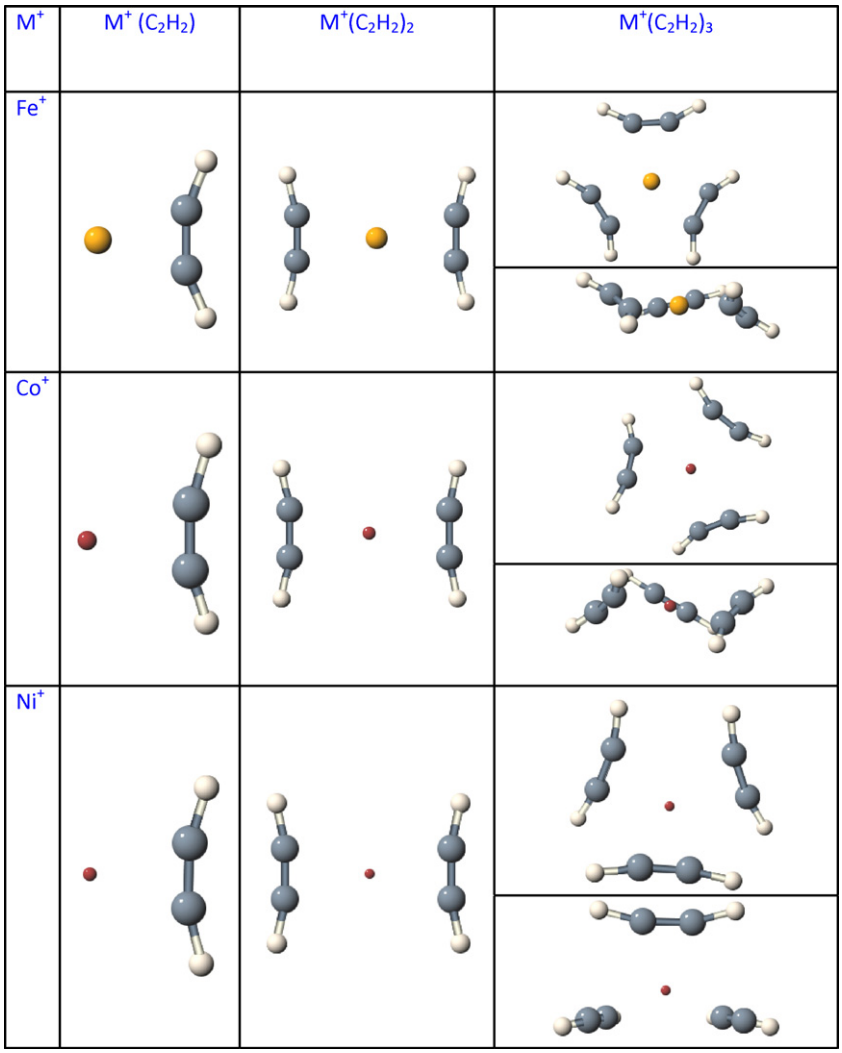

Fig. 11. DFT optimized structures for $M^+(C_2H_2)_n$ complexes (n = 1–3). Optimizations were performed with B3LYP utilizing the Wachters + f basis set. See Supplementary data, Tables S1–S3, for binding energies, bond lengths and angles, and C—H vibration frequencies.

all monomer complexes possess a C_{2v} symmetry and $^nB_1$ ground electronic state (Table S1, Supplementary data).

Comparison of the calculated structures, energies and vibrational frequencies to those computed by Klippenstein and Yang [37], Duncan and co-workers [49], and Sicilia and Russo [48] show reasonable agreement (Table S1, SI). The only discrepancy is the calculated ground state of $Fe^+(C_2H_2)$ to be $^4B_1$ and not $^4B_2$ as with previous investigations [37,50]. Also, our calculated binding energy for this complex (50.0 kcal/mol) is larger than previously predicted (42.6 kcal/mol, Table S1, Supplementary data). We attribute this discrepancy to the failure of the basis set (Wachters + f) to properly describe the iron cation tendency to change electronic state (spin) in going from the bare ion to the complexed one. Klippenstein and Yang [37] using a different basis set described a similar problem. For the other metals (Co^+ and Ni^+) where spin is conserved, the Wachters + f basis set yields satisfactory results. It should be pointed out that calculations by Duncan and co-workers [51] using the 6-311+G(3df,2p) basis set also arrived at the same ground electronic state ($^4B_1$) as predicted by the (Wachters + f) basis set here.

As expected, DFT calculations predict planar bis-acetylene geometry for Fe^+, Co^+, and Ni^+/acetylene dimer clusters (Fig. 11). This was expected based on the enhanced intensities observed for the three $M^+(C_2H_2)_2$ clusters (see Fig. 10a–c for TOF mass spectra). Several experimental and theoretical investigations have confirmed the bis-acetylene geometry to be the most stable for iron and nickel/acetylene complexes [27,44,48].

As was the case in the monomer complexes, there was an increase in magnitude of the C—H stretch frequency red shift (compared to that of the neutral acetylene molecule) from nickel to iron resulting from increasing σ-electron donation from acetylene to the metal d-orbital and back-donation of π-electron density to the π^*-orbital of acetylene. Binding energy (D_e) for the removal of an acetylene molecule D_e [$M^+(C_2H_2)$–(C_2H_2)] was 33.4, 35.4, and 37.8 kcal/mol for $M^+ = Fe^+$, Co^+ and Ni^+, respectively (Table S2, Supplementary data). The reduction in binding energy as compared to the monomer complexes is due to the interaction between the acetylene molecules.

Optimized geometries for the $M^+(C_2H_2)_3$ clusters for Fe^+ and Co^+, show a pseudo-cyclic structure with each acetylene molecule distorted from planarity (Fig. 11) to reduce repulsive interaction between ligands (predicted symmetries were D_3 and C_3 for $Fe^+(C_2H_2)_3$ and $Co^+(C_2H_2)_3$, respectively). The predicted geometry for the Ni^+ trimer complex differs markedly from those of Fe^+ and Co^+. Instead of the pseudo-cyclic structure, the $Co^+(C_2H_2)_3$ geometry (C_s) is basically an addition of a third acetylene molecule to the "puckered" geometry predicted for the dimer complex. The third acetylene molecule is located above the dimer plane with CCH angles (165.4°) different from the other two acetylene molecules

(167.4°/168.8°) (Table S3, Supplementary data). For all three TM ion trimer complexes $Fe^+(C_2H_2)_3$, $Co^+(C_2H_2)_3$ and $Ni^+(C_2H_2)_3$, the metal cation is embedded in a "cage" created by the three acetylene molecules..

4. Discussion

The generation of hydrocarbon fragments with different composition and intensity from the reactions of TM ions and acetylene clusters could suggest a varying order of catalytic activity of the TM ions towards polymerization of acetylene. Since in the mass spectra we also observe hydrogen abstracted acetylene clusters (catalyzed by metal ion), it can be assumed that the fragment ions are produced upon reactions of the TM ions within the clusters followed by evaporation from the clusters. Based on the abundance of the ions namely $C_6H_4^+$, $C_6H_5^+$, $C_8H_6^+$ and $C_8H_7^+$ it can be concluded that these ions are covalently bonded hydrocarbons and not simply composed of acetylene clusters bound by ion-induced dipole and dispersion interactions. These fragment ions are suspected products of TM cation induced cyclotrimerization of acetylene to form the benzene ion, $C_6H_6^+$, and its fragment product ions, $C_6H_5^+$ and $C_6H_4^+$, as previously reported by Schwarz and co-workers in the case of Fe^+ [26–28]. We have shown in earlier studies that EI ionization of large acetylene clusters produces a prominent ion signal at $(C_2H_2)_3^+$ with a structure identical to that of the benzene cation generated as a result of intracluster ion–molecule reactions [41]. Another study, based on vibrational predissociation spectroscopy, has suggested the presence of multiple isomers of the $(C_2H_2)_3^+$ ion including a contribution from the benzene type ion in cationic acetylene clusters $(C_2H_2)_n^+$ formed by charge-transfer collisions of Ar^+ with neutral acetylene clusters [52]. We have also reported new reactions of the benzene radical cation with acetylene over a wide temperature range from 120 K to 680 K, showing that acetylene undergoes sequential additions onto the benzene cation with two different mechanisms operating at low and high temperatures [53]. Interestingly, under ordinary conditions at 300 K, the benzene cation does not react with acetylene as reported by another study [54]. However, at low temperatures (120 K) associative charge transfer reactions of acetylene onto the benzene cation catalyze the conversion of acetylene molecules into cyclic/polymerized ions. At high temperatures (680 K) addition/elimination reactions lead to the generation of possible naphthalene-type ions [52].

Since in the present work the major hydrocarbon ions observed are due to $C_6H_4^+$, $C_6H_5^+$, $C_8H_6^+$ and $C_8H_7^+$, it appears that the observation of these ions in the mass spectra is a signature of a metal ion catalyzed polymerization process distinct from the reactions observed in cationic acetylene clusters $(C_2H_2)_n^+$ [41,52–54]. Previous studies dealing with gas phase reactions of TM cations with acetylene have reported cyclotrimerization of acetylene resulting in the formation of $C_6H_6^+$ [26–28]. In the present study, $C_6H_6^+$ is not a major ion but the related ions $C_6H_4^+$ and $C_6H_5^+$ and the higher analogs $C_8H_6^+$ and $C_8H_7^+$ are observed following the reactions of laser-generated Fe^+, Co^+ and Ni^+ ions with neutral acetylene clusters.

Based on previous studies on the reactivity of TM ions with small organic molecules, it has been inferred that first row group 8–10 metal ions are more active towards C—C bond activation, whereas the metal ions early in the transition series, as well as the second- and third-row metal ions preferentially activate the C—H bonds [55]. This is also clearly evident from the mass spectra of the $V^+(C_2H_2)_n$ clusters (Fig. 3) which shows significant hydrogen abstraction of the type $VC_{2n}H_{2n-m}^+$, thus suggesting that these species are produced by the C—H bond activation of the metal ion–acetylene complexes. This observation suggests that the mechanism responsible for TM initiated polymerization of acetylene clusters, under our experimental conditions proceeds via C—H bond activation.

4.1. Mechanism for catalytic polymerization of acetylene

Under the current experimental conditions, we were unable to detect any ion signal when the focused laser beam was allowed to directly interact with the supersonic jet of acetylene clusters. On the other hand, strong ion signals corresponding to the metal–acetylene cluster ions and other hydrocarbon fragments were readily observed when the produced clusters interacted with metal cations generated by LVI. The observation of dehydrogenated acetylene cluster ions of the type $C_{2n}H_{2n-m}^+$ in the mass spectra suggests that these ions originate from the metal–acetylene cluster ions and are produced as a result of a cluster evaporation process. Also since the observation of hydrocarbon ions depends on the nature of the TM cation under identical experimental conditions, the possibility of acetylene polymerization by EI ionization of neutral clusters using energetic electrons produced by LVI process is unlikely.

It is well known that TM ions are characterized by a large number of low-lying electronic states that can be easily accessed under the typical LVI conditions [40,56,57]. Since most of the low-lying electronic states of first-row TM cations have either a $3d^n$ or a $4s^1 3d^{n-1}$ electronic configuration, most of the transitions between these states are parity forbidden. Therefore, the radiative life times of the excited states can be on the order of milliseconds or even seconds which allow the experimental observation of these states [58]. In fact, ion mobility measurements for most of the laser-generated transition metal cations reveal the presence of two or three mobility peaks that correspond to ground and excited states of different electronic configurations [40]. It has been shown that the LVI process under conditions similar to the current experimental conditions can easily access excited states with energies in the range of 1–1.5 eV [40]. It is interesting that the observed reactivity of the TM cations towards acetylene cluster polymerization correlates with the presence of low-lying electronic states. For example, the TM cations V^+, Fe^+, Co^+ and Ni^+ have several excited states lying within 1.2 eV of their ground states as shown in Table S4 (Supplementary data) [40,56]. In the present work, hydrogen abstraction reactions (Eq. (1)) are observed in $V^+(C_2H_2)_n$ (Fig. 3, inset), and efficient generation of hydrocarbon ions is observed within $Fe^+(C_2H_2)_n$, $Co^+(C_2H_2)_n$ and $Ni^+(C_2H_2)_n$ clusters (Figs. 5–7). On the other hand, no reactivity is observed in acetylene clusters containing Cr^+, Cu^+ and Zn^+ ions where their first excited states energies are 1.52, 2.81 and 7.9 eV, respectively [56]. This correlation suggests that the observed C—H bond activation is driven by electronically excited TM ions possessing low-lying excited states that can be reached under the current LVI conditions. In our experiments, the $M^+(C_2H_2)_n$ clusters are generated by the pickup method, and it is expected that the excited metal ion would reside on the surface of the acetylene clusters for significant duration for the C—H activation to take place. Based on the observed fragmentation pattern, it is clear that the fragment $C_4H_3^+$ is an essential link to the generation of species such as $C_6H_4^+$, $C_6H_5^+$, $C_8H_6^+$ and $C_8H_7^+$. The catalytic process could be initiated by C—H bond activation of a surface acetylene molecule on the cluster by the excited metal ion via the formation of an insertion intermediate within the $M(C_2H_2)_n^+$ cluster by oxidative addition. The activated acetylene molecule adds further acetylene units leading to the formation of higher acetylene polymeric ions as shown in Scheme 1.

Scheme 1 qualitatively explains the mechanism of acetylene polymerization resulting in formation of the hydrocarbon fragments $C_4H_3^+$, $C_6H_5^+$ and $C_8H_7^+$ upon cluster evaporation. This mechanism explains the important role of the $C_4H_3^+$ intermediate in the metal ion-assisted acetylene polymerization. The genera-

$$M^{*+}(C_2H_2)_n \longrightarrow [H\text{-}M\text{-}C_2H\cdots(C_2H_2)_{n-1}]^+ \longrightarrow [H\text{-}M\text{-}C_4H_3\cdots(C_2H_2)_{n-2}]^+ \longrightarrow [H\text{-}M\text{-}C_6H_5\cdots(C_2H_2)_{n-3}]^+ \longrightarrow [H\text{-}M\text{-}C_8H_7\cdots(C_2H_2)_{n-4}]^+$$

Scheme 1.

tion of species like $C_6H_4^+$ and $C_8H_6^+$ could be ascribed to β-H abstraction upon activation of additional C—H bond by the metal ion. Also these ions could be produced if the condensation ion is formed with excess energy [59]. Previously, Walch has theoretically investigated the minimum energy pathway for the ring closure reaction of C_4H_3 with C_2H_2 using RHF calculations and concluded that the ring closure reaction leading to phenyl radical formation is thermodynamically favorable [60]. Similarly, Bauschlicher et al. investigated the mechanism of polycyclic hydrocarbon growth by computing the barriers and heats of reactions for the conversion of benzene to naphthalene upon acetylene addition using the B3LYP approach [61]. In their study it was inferred that the cationic synthesis mechanism is thermodynamically more favored. Based on analogy with the above two studies, which predict ring closure to be thermodynamically favorable, we can infer that under our experimental conditions the polymeric species generated $C_6H_4^+$, $C_6H_5^+$ $C_8H_6^+$ and $C_8H_7^+$ have structures equivalent to benzene and styrene derivatives. However, further theoretical studies are essential to justify this proposition.

5. Conclusions

The present study explores the feasibility of utilizing acetylene clusters as model reactors for screening the catalytic activity of laser-generated transition metal ions towards polymerization of acetylene. A sequential addition of acetylene molecules to a metal activated acetylene monomer within the clusters is proposed as a possible mechanism initiated by C—H bond activation. The proposed mechanism suggests the intermediacy of $C_4H_3^+$ in the generation of higher hydrocarbon species such as $C_6H_4^+$, $C_6H_5^+$, $C_8H_6^+$ and $C_8H_7^+$. Based on thermodynamic considerations it is expected that the observed hydrocarbon ions would have cyclic structures equivalent to benzene and styrene fragments.

Enhanced ion intensities have been observed for $V^+(C_2H_2)_2$, $Cr^+(C_2H_2)_2$, $Fe^+(C_2H_2)_4$, $Fe^+(C_2H_2)_4$, $Co^+(C_2H_2)_3$, $Ni^+(C_2H_2)_3$, and $Cu^+(C_2H_2)_3$ consistent with the formation of stable covalent products formed by metal ion catalyzed polymerization of acetylene clusters. DFT calculations identify the structures of the initially formed trimer ion clusters $Fe^+(C_2H_2)_3$, $Co^+(C_2H_2)_3$ and $Ni^+(C_2H_2)_3$ where the metal cation is embedded in a "cage" created by the three acetylene molecules. Isomerization of these cluster ions into the more stable metal ion–benzene adducts is suggested and the energy needed to surpass the isomerization barriers is likely to come from the laser-generated excited state metal ions. A remarkable even–odd alternation has been observed for $Co^+(C_2H_2)_n$ clusters with enhanced ion intensities for $n = 3$, 6, 9 and 12, which could be explained by multiple isomerization events resulting in the formation of $Co^+(\text{benzene})_n$ clusters with $n = 1$–4. The combination of the excited state energy of the TM ions and the unique cluster environment which promotes concerted multi-monomer interactions with the metal ions could lead, under favorable conditions, to TM ion-mediated cyclotrimerization of acetylene molecules resulting in the formation of benzene and other polycyclic aromatic hydrocarbons. In addition to the formation of covalent adducts, a magic number behavior has been observed for $M^+(C_2H_2)_n$ clusters for M = Fe, Co and Ni and $n = 14$ suggesting the possibility of a cage structure containing a strongly bound $M^+(C_2H_2)_2$ cation core surrounded by 12 neutral acetylene molecules in an icosahedral arrangement. Further experimental and theoretical investigations focusing on the structures of the observed magic numbers are needed to shed more light on metal ion-containing acetylene clusters.

Acknowledgments

We thank the National Science Foundation (CHE-0911146) and NASA (NNX08AI46G) for the support of this work.

Appendix A. Supplementary data

Supplementary data associated with this article can be found, in the online version, at doi:10.1016/j.ijms.2010.10.010.

References

[1] Y.L. Teng, Q. Xu, J. Phys. Chem. A 113 (2009) 12163.
[2] D.K. Bohme, H. Schwarz, Angew. Chem. Int. Ed. 44 (2005) 2336.
[3] M.D.C. Michelini, N. Russo, E. Sicilia, Inorg. Chem. 43 (2004) 4944.
[4] A. Irigoras, J.E. Fowler, J.M. Ugalde, J. Am. Chem. Soc. 121 (1999) 8549.
[5] Y.B. Pithawalla, M.S. El-Shall, Gas phase and cluster studies of the early stages of cationic polymerization and the reactions with metal cations, in: M.O. Hunt, T.E. Long (Eds.), Solvent-Free Polymerizations and Processes, ACS Symposium Series 713, 1998, pp. 232–245 (Chapter 15).
[6] G.M. Daly, Y.B. Pithawalla, Z. Yu, M.S. El-Shall, Chem. Phys. Lett. 237 (1995) 97.
[7] G.M. Daly, M.S. El-Shall, J. Phys. Chem. 98 (1994) 696.
[8] P.A.M. van Koppen, M.T. Bowers, C.L. Haynes, P.B. Armentrout, J. Am. Chem. Soc. 120 (1998) 5704.
[9] P.B. Armentrout, Acc. Chem. Res. 28 (1995) 430.
[10] P.B. Armentrout, Annu. Rev. Phys. Chem. 41 (1990) 313.
[11] K. Eller, H. Schwarz, Chem. Rev. 91 (1991) 1121.
[12] M.S. El-Shall, Acc. Chem. Res. 41 (2008) 783.
[13] Y.P. Ma, W. Xue, Z.C. Wang, M.F. Ge, S.G. He, J. Phys. Chem. A 112 (2008) 3731.
[14] T.J. Katz, S.J. Lee, J. Am. Chem. Soc. 102 (1980) 422.
[15] L.K. Johnson, C.M. Killian, M. Brookhart, J. Am. Chem. Soc. 117 (1995) 6414.
[16] J. Allison, Prog. Inorg. Chem. 34 (1986) 627.
[17] S.W. Buckner, B.S. Freiser, Polyhedron 7 (1988) 1583.
[18] M.T. Bowers, Acc. Chem. Res. 27 (1994) 324.
[19] B.S. Freiser, Acc. Chem. Res. 27 (1994) 353.
[20] M.C. Holthausen, A. Fiedler, H. Schwarz, W. Koch, Angew. Chem. Int. Ed. Engl. 34 (1995) 2282.
[21] M.C. Holthausen, W. Koch, J. Am. Chem. Soc. 118 (1996) 9932.
[22] J.C. Weisshaar, Acc. Chem. Res. 26 (1993) 213.
[23] T.F. Magnera, D.E. David, J. Michl, J. Am. Chem. Soc. 109 (1987) 936.
[24] J.B. Schilling, J.L. Beauchamp, J. Am. Chem. Soc. 110 (1988) 15.
[25] P. Mourgues, A. Ferhati, T.B. McMahon, G. Ohanessian, Organometallics 16 (1997) 210.
[26] D. Schröder, D. Sulzle, J. Hrusak, D.K. Bohme, H. Schwarz, Int. J. Mass Spectrom. Ion Processes 110 (1991) 145.
[27] K. Schroeter, C.A. Schalley, R. Wesendrup, D. Schröder, H. Schwarz, Organometallics 16 (1997) 986.
[28] R. Wesendrup, H. Schwarz, Organometallics 16 (1997) 461.
[29] S. Chrétien, D.R. Salahub, J. Chem. Phys. 119 (2003) 12291.
[30] V. Gevorgyan, U. Radhakrishnan, A. Takeda, M. Rubina, M. Rubin, Y. Yamamoto, J. Org. Chem. 66 (2001) 2835.
[31] M. Martinez, M. del, C. Michelini, I. Rivalta, N. Russo, E. Sicilia, Inorg. Chem. 44 (2005) 9807.
[32] S. Abbet, A. Sanchez, U. Heiz, W.D. Schneider, A.M. Ferrari, G. Pacchioni, N. Rösch, J. Am. Chem. Soc. 122 (2000) 3453.
[33] W.A. de Heer, P. Milani, Rev. Sci. Instrum. 62 (1991) 670.
[34] W. Kohn, L.J. Sham, Phys. Rev. 140 (1965) A1133.
[35] M.J. Frisch, G.W. Trucks, H.B. Schlegel, G.E. Scuseria, M.A. Robb, J.R. Cheeseman, V.G. Zakrzewski, J.A. Montgomery, R.E. Stratmann, J.C. Burant, S. Daprich, J.M. Millam, A.D. Daniels, K.N. Kudin, M.C. Strain, O. Farkas, J. Tomasi, V. Barone, M. Cossi, R. Cammi, B. Mennucci, C. Pomelli, C. Adamo, S. Clifford, J. Ochterski, G.A. Petersson, P.Y. Ayala, Q. Cui, K. Morokuma, D.K. Malick, A.D. Rabuck, K. Raghavachari, J.B. Foresman, J. Cioslowski, J.V. Ortiz, A.G. Baboul, B.B. Stefanov, G. Liu, P. Liashenko, P. Piskorz, I. Komaromi, R. Gomperts, R.L. Martin, D.J. Fox, T. Keith, M.A. Al-Laham, C.Y. Peng, A. Nanayakkara, C. Gonzalez, M. Challacombe, P.M.W. Gill, B.G. Johnson, W. Chen, M.W. Wong, J.L. Andres, C. Gonzalez, M. Head-Gordon, E.S. Replogle, J.A. Pople, *Gaussian 03*, revision C.02, Gaussian, Inc, Pittsburgh, PA, 2004.
[36] I. Bytheway, M.W. Wong, Chem. Phys. Lett. 282 (1998) 219.
[37] S.J. Klippenstein, C.N. Yang, Int. J. Mass Spectrom. 201 (2000) 253.
[38] C.B. Lebrilla, C. Schulze, H. Schwarz, J. Am. Chem. Soc. 109 (1987) 98.

[39] M. Rosi, C.W. Bauschlicher Jr., Chem. Phys. Lett. 166 (1990) 189.
[40] Y. Ibrahim, E. Alsharaeh, R. Mabrouki, P. Momoh, E. Xie, M.S. El-Shall, J. Phys. Chem. A 112 (2008) 1112–1124.
[41] P.O. Momoh, S.A. Abrash, R. Mabrouki, M.S. El-Shall, J. Am. Chem. Soc. 128 (2006) 12408.
[42] A.W. Castleman, S. Wei, Annu. Rev. Phys. Chem. 45 (1994) 685.
[43] A.W. Castleman Jr., K.H. Bowen Jr., J. Phys. Chem. 100 (1996) 12911.
[44] R.S. Walters, T.D. Jaeger, M.A. Duncan, J. Phys. Chem. A 106 (2002) 10482.
[45] O. Ingolfsson, A.M. Wodtke, J. Chem. Phys. 117 (2002) 3721.
[46] T.P. Martin, T. Bergmann, H. Goehlich, T. Lange, J. Phys. Chem. 95 (1991) 6421.
[47] I.L. Alberts, T.W. Rowlands, N.C. Handy, J. Chem. Phys. 88 (1988) 3811.
[48] E. Sicilia, N. Russo, J. Mol. Struct. (Theochem.) 709 (2004) 167.
[49] R.S. Walters, E.D. Pillai, P.V.R. Schleyer, M.A. Duncan, J. Am. Chem. Soc. 127 (2005) 17030.
[50] M. Sodupe, C.W. Bauschlicher Jr., J. Phys. Chem. 95 (1991) 8640.
[51] R.S. Walters, P.V.R. Schleyer, C. Corminboeuf, M.A. Duncan, J. Am. Chem. Soc. 127 (2005) 1100.
[52] R.A. Relph, J.C. Bopp, J.R. Roscioli, M.A. Johnson, J. Chem. Phys. 131 (2009) 114305.
[53] P.O. Momoh, A.R. Soliman, M. Meot-Ner, A. Ricca, M.S. El-Shall, J. Am. Chem. Soc. 130 (2008) 12848.
[54] D.K. Bohme, S. Wlodek, J.A. Zimmerman, J.R. Eyler, Int. J. Mass Spectrom. Ion Processes 109 (1991) 31.
[55] S.W. Buckner, T.J. MacMahon, G.D. Byrd, B.S. Freiser, Inorg. Chem. 28 (1989) 3511.
[56] P.R. Kemper, M.T. Bowers, J. Phys. Chem. 95 (1991) 5134.
[57] M.T. Bowers, P.R. Kemper, G. von Helden, P.A.M. Van Koppen, Science 260 (1993) 1446.
[58] J.L. Elkind, P.B. Armentrout, J. Phys. Chem. 89 (1985) 5626.
[59] V.G. Anicich, A.D. Sen, W.T. Huntress Jr., M.J. McEwan, J. Chem. Phys. 93 (1990) 7163.
[60] S.P. Walch, J. Chem. Phys. 103 (1995) 8544.
[61] C.W. Bauschlicher Jr., A. Ricca, Chem. Phys. Lett. 326 (2000) 283.